

POROSITY OF POLISHED GLAZES OBTAINED BY DRY APPLICATION

A. Escardino⁽¹⁾, M.J. Orts⁽¹⁾, A. Gozalbo⁽¹⁾, S. Mestre⁽¹⁾
J. F. Aparisi⁽²⁾, F.J. Ferrando⁽²⁾, A. J. Ramos⁽²⁾, L.F. Sánchez⁽²⁾

⁽¹⁾Instituto de Tecnología Cerámica. Asociación de Investigación de las
Industrias Cerámicas. Universitat Jaume I. Castellón. España

⁽²⁾ESMALGLASS, S.A.

ABSTRACT

In this study a method has been fine-tuned to determine the porosity of polished glazes when porosity is very low (less than 1% polished surface occupied by pores). A study has been undertaken, in glazes obtained by dry application of frits in the form of grit, of the effect of glazed tile constituents (body, base glaze and grit) and the thermal cycle used on polished glaze porosity. The study has been conducted with industrial size tiles, fired in a pilot roller kiln.

1. INTRODUCTION

When glazed tiles are polished, occluded pores in the glaze layer appear at the surface, deteriorating product quality. Pore size and quantity are determined by different factors^[1]: packing of the unfired layer of glaze particles, possible devitrifications during firing, reactivity of the glaze with the body, gas retention, etc. Although the combination of all these factors makes it practically impossible to entirely eliminate glaze porosity, certain actions can be adopted to minimise glaze porosity.

Studies have shown that glaze porosity is very low when glazes are made from raw materials of a glassy nature without devitrifications during firing. In fact, when glaze is applied by the wet method, fired glaze porosity can approach 2%, with pore sizes of the order of 10µm if transparent frits of the so-called crystalline type are used, which do not devitrify with heat treatment^[2].

If a dry frit application in the form of grit is involved, of a particle size between 200 and 500µm, the frit particles soften and deform during firing, rearranging themselves and filling the interparticle voids. This leads to glazes of less than 0.5% porosity.

Because of the low porosity of glazes obtained by applying dry grits, it is not advisable to measure porosity on polished glaze cross sections, since these often contain no pores. Surface measurement is therefore required.

The present paper sets out the results obtained on studying the effect of certain process variables on the outer porosity of glazes produced by dry application of two frits in the form of grit. For this, industrial porcelain tile bodies were used that were coated with a base glaze layer, which was applied wet, a screen print and a dry frit application in the form of grit. The pieces were fired in a pilot roller kiln with four different thermal cycles. Three types of body and two base glazes of different nature were tested with each frit.

2. EXPERIMENTAL

The bodies used have been referenced S1, S2 and S3, the two glaze suspensions E1 and E2, and the two tested frits G1 and G2. Unfired porcelain tile bodies were used, measuring 41x4cm, whose dry bulk densities are detailed in Table 1.

Body	Dry bulk density (g/cm ³)
S1	1.916
S2	1.972
S3	1.951

Table 1. Dry bulk densities of the bodies used.

The glaze suspensions were mixtures of frit and crystalline materials, milled to industrial application conditions. Suspension E1 contained a barium matt frit and suspension E2 a zirconium white frit.

Mean frit particle size for dry application as grit was 300µm. The two tested frits gave rise to transparent glazes, although frit G1 was more fluxing than frit G2.

A base glaze coat was applied onto the bodies followed by a screen printing decoration, to enable evaluating the transparency of the resulting glazes. The frit was applied dry as grit on the screen printing decoration. Each base glaze was applied onto each type of body, and each frit onto each base glaze, yielding the set of test pieces detailed in Table 2.

Piece	1	2	3	4	5	6	7	8	9	10
Body	S1	S2	S1	S2	S1	S2	S1	S2	S3	S3
Base glaze	E1	E1	E2	E2	E1	E1	E2	E2	E2	E2
Grit	G1	G1	G1	G1	G2	G2	G2	G2	G1	G2

Table 2. Constituents of the prepared test pieces.

The pieces were fired in a pilot roller kiln using four different thermal cycles similar to the cycles used in industry. Cycle peak temperatures and times are detailed in Table 3.

Cycle	Peak temperature (°C)	Total cycle time (min)
C1	1175	75
C2	1200	50
C3	1200	75
C4	1155	75

Table 3. Tested thermal cycles.

The presence of surface defects was estimated visually in the resulting glazes, in addition to determining the apparent porosity of the polished glaze and observing glaze microstructure with a scanning electron microscope.

Porosity of the polished glazed surface was measured with an image analyser connected to an optical microscope, using test specimens measuring 2.5x2.5cm cut from the centre of the test pieces. A laboratory polishing facility was used to polish the glaze. Polishing was performed until 50% of the initial glaze thickness had been removed. Initial glaze thickness was between 700 and 900 μ m. The degree of advance of the polishing operation was controlled with a stereoscopic microscope. The measurement was made on an area of 4cm² in the centre of the test pieces. In addition to porosity (expressed as percentage of measured surface area occupied by pores), mean pore diameter was determined in all the test specimens.

In order to verify whether the results obtained were representative, in some of the pieces, glaze porosity was also determined in samples cut from one side. These results were compared with the data of the samples cut from the centre of the piece. The results were found to be the same.

Visual examination of the resulting glazes showed that the same combination of base glaze and grit led to different results, depending on the type of body used.

The three bodies were therefore characterised, determining particle and pore-size distribution of the unfired bodies, and conducting chemical, mineralogical and thermogravimetric analysis of these bodies. Fired bulk density was also determined in bodies fired with one of the cycles (C1) and their microstructure was observed with a scanning electron microscope.

To study the possible influence of the base glaze on polished glaze porosity, pieces of body S3 with respective applications of base glazes E1 and E2 were fired in an electric laboratory kiln. The firing cycle used was the standard one for floor tile bodies and the peak firing temperatures tested were 1180, 1200 and 1220°C. Polished cross sections of the fired pieces were prepared and glaze microstructure was observed.

The combined effect of base glaze and body was studied by applying three suspensions of frit, referenced F1, F2 and F3; firing yielded a barium matt glaze, a zirconium white glaze and a transparent glaze, respectively. The three glaze suspensions were applied onto industrial porcelain tile body S2 and onto pieces formed by pressing a standard spray-dried powder used in porcelain tableware manufacture at a pressure of 400 kg/cm², with a powder moisture content of 5.5%. The resulting test specimens were fired in an electric laboratory kiln using a typical porcelain tile cycle at peak temperatures of 1200 and 1220°C, then visually estimating the number of defects (pinholes and dimples) contained in the glazed surfaces.

3. RESULTS

3.1. POROSITY AND MEAN PORE DIAMETER OF THE POLISHED GLAZES

Apparent (surface) porosity of the polished glazes and mean diameter of the surface pores are set out in Tables 4 and 5, respectively. In these tables, Ci refers to the thermal cycle used to fire the test pieces (C1 to C4). It can be observed that the polished surface of the studied glazes exhibits very low porosity, compared with that of polished glazes made by wet application, whose minimum value lies around 2% in the case of the so-called crystalline glazes which have the lowest porosity after polishing^[2].

Porosity and pore size of all the glazes prepared with the C1 cycle have been determined, regardless of whether the surface displayed pinholes or not before polishing, with a view to having a complete series of pieces. In the pieces fired with cycles C2, C3 and C4, the glazes exhibiting pinholes were not measured.

Table 4 shows that the thermal cycle hardly influences the porosity of a given glaze in the tested range, so that in order to analyse the influence of the constituents of the pieces, the arithmetic mean has been calculated of the four values obtained with each glaze. Table 6 details these mean values, in order of increasing porosity. In this table, the glazes marked with an asterisk displayed pinholes across the entire surface, and these were the most porous.

Following the same criterion, the arithmetic mean was also determined of the mean pore size values for each glaze. Table 7 lists these mean values, in increasing order.

Piece	Constituents	ϵ (%)			
		C4 (1155°C,75min)	C1 (1175°C,75min)	C2 (1200°C,50min)	C3 (1200°C,75min)
Ci-1	S1-E1-G1	0.24	0.29	0.23	0.21
Ci-2	S2-E1-G1	0.27	0.35 ⁺	(*)	(*)
Ci-3	S1-E2-G1	0.26	0.28	0.21	0.22
Ci-4	S2-E2-G1	(*)	0.51 ⁺	(*)	(*)
Ci-5	S1-E1-G2	0.25	0.28	0.21	0.23
Ci-6	S2-E1-G2	0.27	0.28 ⁺	(*)	(*)
Ci-7	S1-E2-G2	0.26	0.26	0.19	0.24
Ci-8	S2-E2-G2	(*)	3.29 ⁺	(*)	(*)
Ci-9	S3-E2-G1	0.29	0.33	0.35	0.31
Ci-10	S3-E2-G2	0.39	0.43	0.33	0.30

(*) No measurement was made (original surface with widespread pinholing).

⁺ Measurement performed though the original surface contained widespread pinholing.

Table 4. Porosity (ϵ) of the polished glazes made with the four test thermal cycles.

Piece	Constituents	d_{50} (μm)			
		C4 (1155°C,75min)	C1 (1175°C,75min)	C2 (1200°C,50min)	C3 (1200°C,75min)
Ci-1	C1-E1-G1	19.7	48.0	39.9	36.2
Ci-2	S-E1-G1	30.6	50.4 ⁺	(*)	(*)
Ci-3	C-E2-G1	24.1	35.3	39.9	24.0
Ci-4	S-E2-G1	(*)	114.6 ⁺	(*)	(*)
Ci-5	C-E1-G2	62.5	72.63	72.5	60.5
Ci-6	S-E1-G2	68.7	80.8 ⁺	(*)	(*)
Ci-7	C-E2-G2	61.1	61.4	67.6	60.8
Ci-8	S-E2-G2	(*)	639.0 ⁺	(*)	(*)
Ci-9	P-E2-G1	31.1	28.9	40.7	28.3
Ci-10	P-E2-G2	57.6	76.5	75.2	67.8

(*) No measurement was made (original surface with widespread pinholing).

⁺ Measurement performed though the original surface contained widespread pinholing.

Table 5. Mean pore diameter (d_{50}) of the polished glazes obtained with the four test thermal cycles.

Piece	Mean porosity (%)	Base	Grit	Body
Ci-7	0.24	E2	G2	S1
Ci-5	0.24	E1	G2	S1
Ci-3	0.24	E2	G1	S1
Ci-1	0.25	E1	G1	S1
Ci-9	0.32	E2	G1	S3
Ci-10	0.36	E2	G2	S3
Ci-6	0.28*	E1	G2	S2
Ci-2	0.31*	E1	G1	S2
Ci-4	0.51*	E2	G1	S2
Ci-8	3.29*	E2	G2	S2

* Pieces exhibiting pinholes.

Table 6. Mean values of glaze porosity.

Piece	d_{50} (μm)	Base	Grit	Body
Ci-3	31	E2	G1	S1
Ci-9	32	E2	G1	S3
Ci-1	36	E1	G1	S1
Ci-2	41	E1	G1	S2
Ci-7	63	E2	G2	S1
Ci-5	67	E1	G2	S1
Ci-10	69	E2	G2	S3
Ci-6	75	E1	G2	S2
Ci-4	115	E2	G1	S2
Ci-8	639	E2	G2	S2

Table 7. Mean values of glaze mean pore diameter.

Table 6 shows that the body has a pronounced influence on glaze porosity. The lowest porosity was obtained with body S1, followed by body S3, while body S2 produced very porous glazes with numerous pinholes. In this table, no clear influence can be observed of the base glaze or the grit on porosity, except in the case of the pieces with body S2, where the combination of this body with base glaze E2 produces the most porous glazes.

With regard to pore size (Table 7), this is also influenced by the nature of the body, and is much greater in the glazes obtained on body S2. Again, the combination of body S2 with base glaze E2 leads to glazes with the largest pores. In the glazes obtained on the other two bodies, an influence of the base glaze is

not observed. Comparison of the porosity values in the glazes corresponding to the pieces with the same body shows that grit G2 always generates larger pores than G1.

As indicated above, the firing cycle does not appear to influence porosity or pore size significantly in the glazes made, except in the case of the pieces obtained with the combination of body S2 and base glaze E1. At higher temperature cycles (C1, C2, C3), this tile glaze displays numerous pinholes which do not form in the lower firing temperature cycle (C4).

3.2. INFLUENCE OF THE BODY ON POROSITY AND PORE SIZE OF THE POLISHED GLAZES

The results obtained show that the body affects the porosity of the glazes made by dry grit application. In the case of glazes produced by wet frit application^[2], owing to their greater porosity, the variation of this property, which is caused by the change in nature of the body, lies within the range of absolute error of the measurement.

Visual comparison of the microstructure of the three bodies fired using the same thermal cycle (cycle C1) shows that they do not exhibit the same densification (Figure 1). This result is confirmed when the bulk densities of the bodies fired with thermal cycle C1 (Table 8) are compared, of which body S1 displays the highest bulk density.

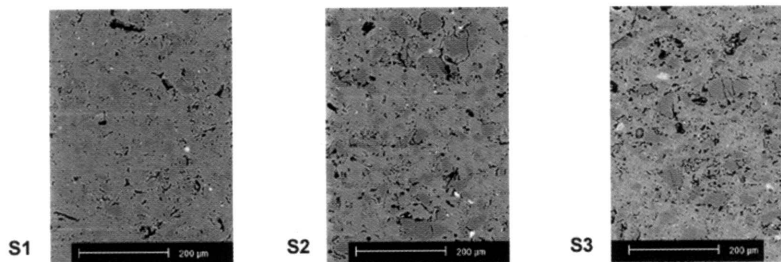


Figure 1. Appearance of the bodies by scanning electron microscopy.

Body	Dry bulk density (g/cm ³)	Fired bulk density (g/cm ³)
S1	1.916	2.364
S2	1.972	2.298
S3	1.951	2.306

Table 8. Dry and fired bulk density of the bodies fired with cycle C1.

To establish the cause of these differences we measured bulk density and pore-size distribution of the three unfired bodies by mercury porosimetry (Figure 2). S1 has the smallest dry bulk density, but the mean pore size is smaller than that of the other two bodies (curve shifted towards the left). This smaller pore size, due to the large fine

particle content^[3] shown in Figure 3, leads to greater densification of the fired product, despite having a lower dry bulk density.

Table 6 shows that the glazes obtained on body S1 have the lowest porosity. A possible reason why S1 leads to less porous glazes could be because ceramic bodies start densifying at lower temperature when the mean pore diameter is smaller. Therefore, densification may be favoured in the case of smaller mean pore diameter at temperatures where the glaze layer is still permeable, allowing the air initially occluded in the pores of the body to evolve through this layer. In accordance with this mechanism, the S2 body would reach the same degree of densification as S1 at higher temperatures, so that a fraction of the air that is eliminated during densification could be retained in the glaze layer, which had lost its permeability.

Figure 4 depicts a cross section of the base glaze-body interface of one of the pieces prepared with body S2 (S2-E2-G1), fired with cycle C3 (higher temperature and longer dwell time). It can be observed how the bubbles of the gas initially present in the voids of the unfired product move from the surface of the body into the base glaze. This movement is facilitated when base glaze melt viscosity decreases.

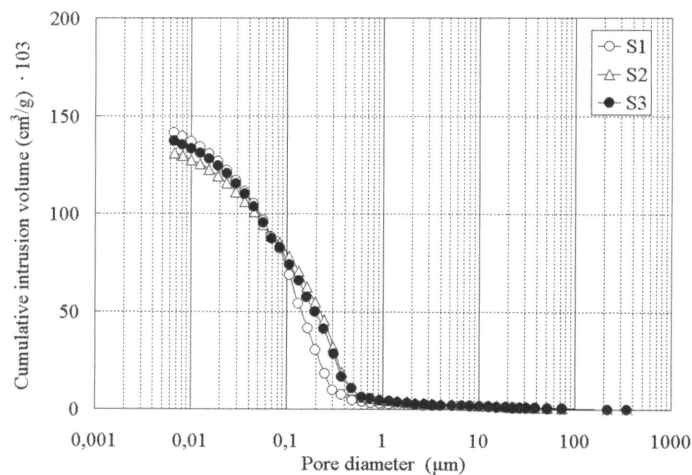


Figure 2. Pore-size distribution of the unfired compacts.

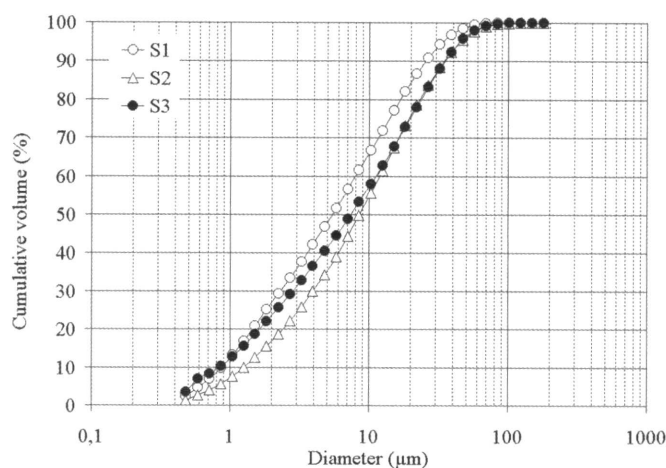


Figure 3. Particle-size distribution of the three body compositions.

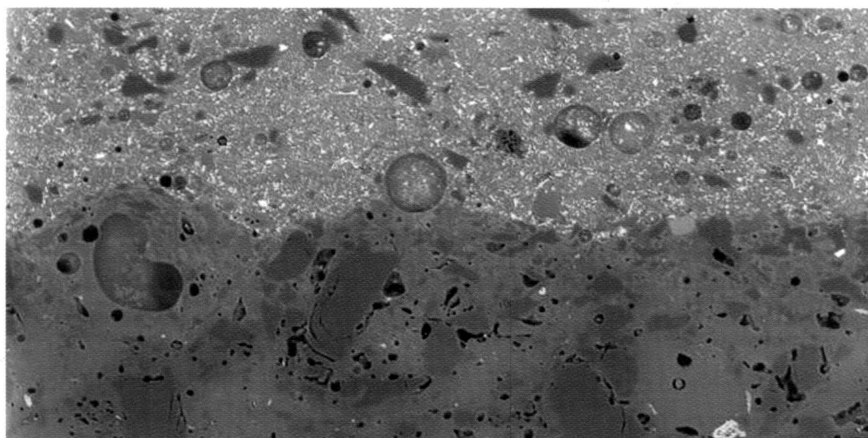


Figure 4. Interface body-base glaze in one of the studied pieces.

In addition to the differences observed between the three tested bodies with regard to dry particle and pore-size distribution, there are also other differences relating to the chemical and mineralogical composition of their constituents.

With regard to chemical composition, to be noted is the 0.98% Fe₂O₃ content of the S2 body as opposed to 0.57% for S1 and 0.37% for S3. Ferric oxide can be reduced to magnetite at high temperatures (by dissociation), releasing oxygen. The greater Fe₂O₃ content in the body could therefore cause greater glaze porosity.

In the diffractograms obtained for the three unfired bodies, quartz, illite, potassium and sodium feldspar and kaolinite were identified. Chlorite was also identified in bodies S1 and S2, and a small percentage of dolomite was detected in S2. The approximate mineralogical compositions were then calculated based on the chemical composition of the bodies and the crystalline phases detected by X-ray diffraction. These are detailed in Table 9. Finally, thermogravimetric analysis was performed on the three bodies. The thermograms show that S2 displays mass loss in the 1000 to 1100°C temperature range, which could be related to its greater hematite content.

	Albite	K feldspar	Illite	Dolomite	Chlorite	Kaolin	Quartz	Others
S1	37	-	13	-	2	21	26	1
S2	19	12	9	2	1	24	32	1
S3	47	3	7	-	1	19	22	1

Table 9. Approximate mineralogical composition (mass%) of the unfired bodies.

3.3. INFLUENCE OF THE NATURE OF THE BASE GLAZE ON POROSITY AND PORE SIZE OF THE RESULTING GLAZES

Figures 5 and 6 correspond to a cross section of the fired pieces showing the microstructure of the base glaze layer, located between that of the glaze (produced from the grit) and the body. The layer obtained from base glaze E1 contains a large quantity of barium aluminosilicate crystals resulting from devitrification of the original frit particles, as well as numerous zircon particles that were already present in the glaze suspension. This glaze is quite reactive and interacts with the screen printing frit and the grit, next to which it forms a region about $38\mu\text{m}$ thick, free of barium aluminosilicate. Such an interaction zone below the screen print is not observed in the layer corresponding to base glaze E2, suggesting that this glaze is less reactive with the screen print than the previous one.

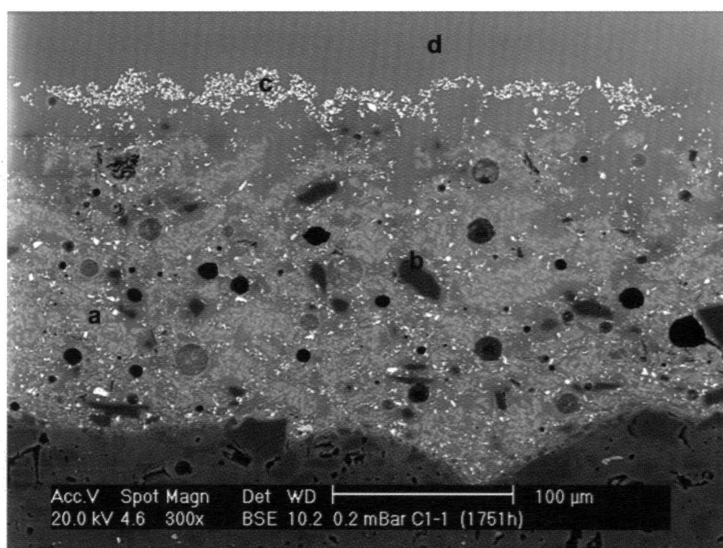


Figure 5. Base glaze E1. a) barium aluminosilicates, b) crystalline material added to the suspension, c) screen print pigment, d) grit G1.

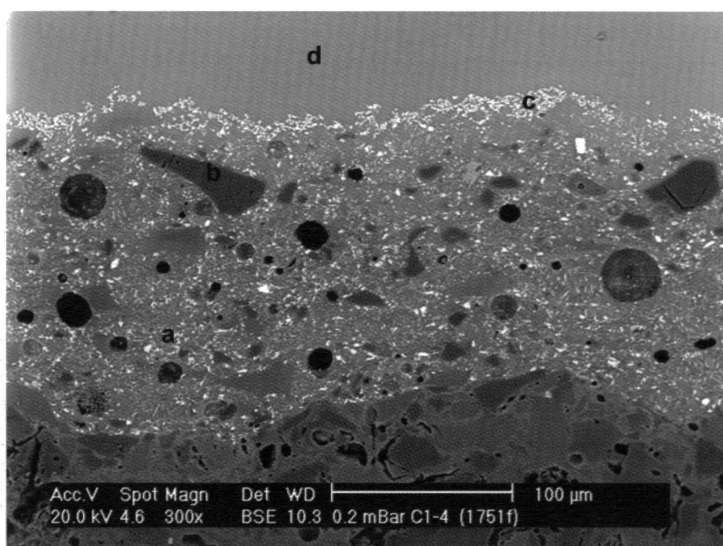


Figure 6. Base glaze E2. a) devitrified zircon, b) crystalline material added to the suspension, c) screen print pigment, d) grit G1.

In order to study the possible effect of the base glaze on apparent porosity of the polished glazes, E1 and E2 suspensions were applied (without applying grit on top) onto the S3 body, which was selected by the collaborating company, and fired in laboratory kiln at peak temperatures of 1180, 1200 and 1220°C. Figure 7 shows a cross section of the glazes produced by firing these coats, using thermal cycles with peak temperatures of 1200 and 1220°C. Base glaze E2 is observed to produce a more porous glaze than E1, with an appreciable rise in porosity and pore size when peak firing temperature is increased from 1200 to 1220°C.

This is because at these maximum temperatures, which are the standard industrial firing temperatures for the studied type of product, E2 base glaze viscosity is lower than that of E1. Consequently, there will probably be gas bubbles that cross the E2 glaze layer and are retained in the top layer of fused grit, which is much thicker.

Barium aluminosilicate crystals devitrify in the layer corresponding to the E1 base glaze. These crystals are relatively large, which considerably increases the effective viscosity of the system^{[4],[5]}, hampering pore growth^[6] and bubble movement inwards into the grit.

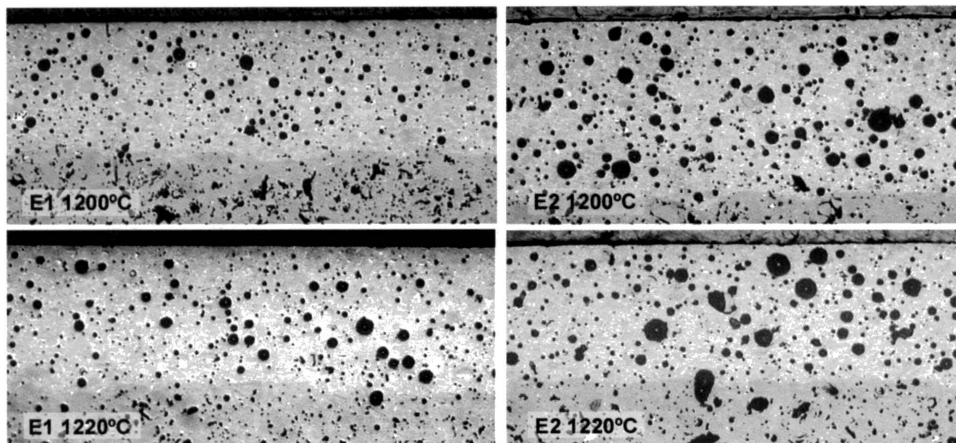


Figure 7. Cross-section of the glazes obtained on applying base glazes E1 and E2 onto body S2 and firing at different temperatures.

Figure 8 shows the appearance of the base glaze-body interface in a cross section of the pieces fired using cycle C4, with bodies S1 and S2, to which base glazes E1 and E2 have been applied. For comparative purposes, the third row also includes micrographs of the microstructure of an inner region of bodies S1 and S2.

In the areas where the S2 body is in contact with the base glazes (micrographs b and d in Figure 8) more glassy phase is observed to form than in the inner body region (micrograph f), owing to greater reactivity with both base glazes; the glaze-body interaction zone appears to be wider in the S2-E2 interface. In contrast, the microstructure of body S1 in the interface with both studied base glazes (micrographs a, c), hardly differs from that of the inner region (e); this result suggests that this body's reactivity with both base glazes is smaller than that of S2. The greater reactivity of S2 could be related to its greater ferric oxide content.

When the ceramic bodies that contain Fe_2O_3 are fired at sufficiently high temperature, this oxide partly dissociates, producing magnetite (Fe_3O_4) and evolving oxygen. If the viscosity of the glaze melt is low, at this temperature, the gas released by the body causes numerous pinholes to form. The magnitude of this phenomenon and the temperature at which it develops depend on the Fe_2O_3 content of the green body and the fusibility of the body. When the reaction develops in the proximity of the base glaze, it will have a pronounced effect on glaze viscosity.

The greater proportion of liquid that forms in the interface can cause the melt in this zone to fill the pores located at the surface of the body, displacing the air into the interior of the glaze. The larger the initial pores of the body (greater particle size in the body), and the higher its reactivity, the more extensive is the pinholing.

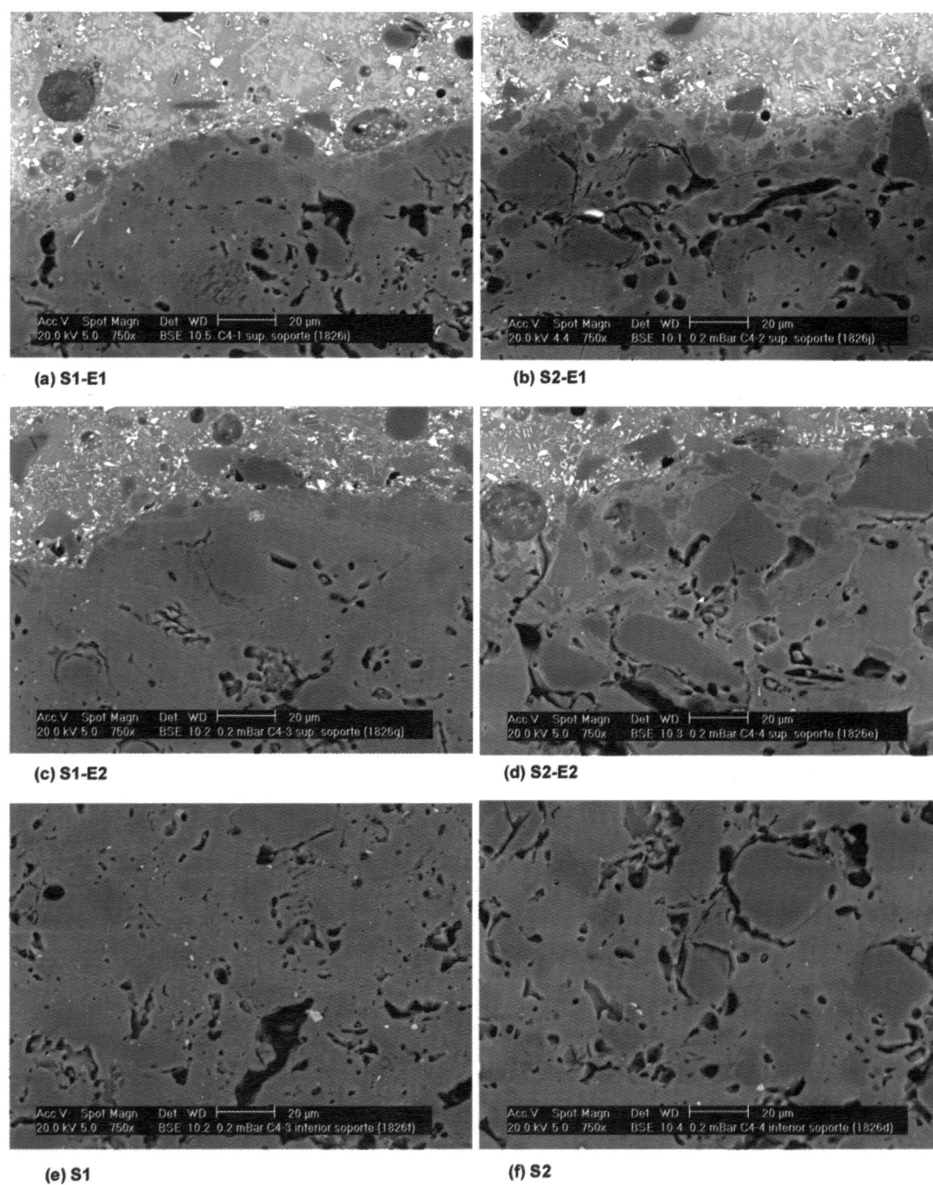


Figure 8. Microstructure of the body of different pieces: (a) S1-E1, (b) S2-E1, (c) S1-E2, (d) S2-E2, (e) inner region of body S1, (f) inner region of body S2.

To confirm the influence of the nature of the body and base glaze on pinhole formation, three glaze suspensions (F1 to F3) were applied onto two different types of unfired body: one porcelain tile body (S2) and another formed from a body customarily used for making porcelain.

Table 10 sets out the results of the visual observation of the glazed surfaces produced after applying glazes F1, F2 and F3 on both bodies and firing these pieces at peak temperatures of 1200 and 1220°C.

It can be observed that matt glaze (F1), whose effective melt viscosity is very high due to its high crystalline phase content, displays no pinholes with the bodies used. In contrast, the surface of the white (F2) and crystalline (F3) glazes, which have a much lower melt viscosity than F1, only exhibit pinholes in the pieces with a porcelain tile body. This phenomenon develops with greater intensity as peak firing temperature rises.

Glaze		Body	Temperature (°C)	
reference	nature		1200	1220
F1	matt	Porcelain tile	no pinholing	no pinholing
		Porcelain	no pinholing	no pinholing
F2	zirconium	Porcelain tile	considerable pinholing	widespread pinholing
	white	Porcelain	no pinholing	no pinholing
F3	transparent	Porcelain tile	considerable pinholing	widespread pinholing
		Porcelain	no pinholing	no pinholing

Table 10. Glazed surface of the pieces.

3.4. EFFECT OF THE FRITS APPLIED AS GRITS

The results obtained with the studied grits (Tables 6 and 7) indicate that the nature of the grit does not appear to influence resulting glaze porosity. However, grit nature does appear to have a considerable effect on pore size. The glazes with the largest pores were obtained with G2, in all likelihood due to its greater surface tension^[7], which would cause bubbles to grow when temperature increased.

3.5. INFLUENCE OF THE THERMAL CYCLE.

As indicated in section 3.1 (please see Table 4), in the set test conditions, for the same base glaze, body and grit, firing cycle peak temperature hardly appears to influence porosity or pore size. However, it is to be noted that two of the tiles prepared with body S2 (S2-E1-G1 and S2-E1-G2) display no pinholes in the firing cycle with the lowest peak temperature (C4). When peak firing temperature and/or dwell time at this peak temperature is raised, all the tiles prepared with body S2 develop pinholes.

Figure 9 shows that the E2 base glaze interacts more intensely with the body than the E1 base glaze in the C4 firing cycle, which could lead to pinholing just in the

S2-E2 pieces with this firing cycle. As peak temperature rises, the E2 base glaze reacts even more strongly with the body, raising the number of pinholes. In contrast, base glaze E1 hardly appears to interact with the body in any of the tested thermal cycles. When peak firing temperature rises, body sintering increases, displacing the gas initially existing in the pores inwards into the molten base glaze and encouraging pinhole formation.

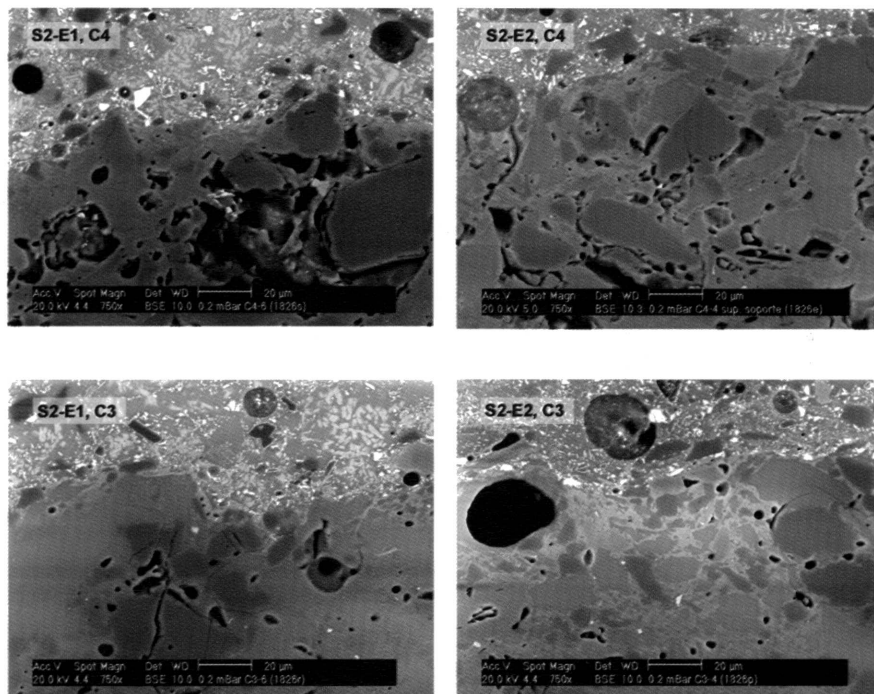


Figure 9. Effect of the thermal cycle on the interface between body S2 and bases E1 and E2.

4. CONCLUSIONS

The study enables drawing the following conclusions:

It has been observed that part of the porosity of these glazes is the result of outgassing of the body. The gas evolving from the body can proceed from decomposition of the ferric oxide initially contained in the body and/or may involve displaced air, as a result of body sintering, as a result of elimination of the pores initially present.

The thermal cycle, in the set test conditions, does not affect porosity or mean pore size in the studied series of glazes.

The glazes with greater porosity have been obtained with the base glaze whose viscosity is lower at the tested peak temperatures. The glaze with the greatest porosity has been obtained with the grit whose composition produces the highest melt surface tension, causing more bubbles to be retained inside the melt.

Pore size rises as body outgassing increases, base glaze melt viscosity decreases and fused grit surface tension at peak firing temperature rises.

The results obtained indicate that if an appropriate body is used (S1 type, for example), with a base glaze of high melt viscosity (like E2) and grit of an analogous nature to G1, tiles can be obtained with glazes of very low porosity.

REFERENCES

- [1] ALVAREZ-ESTRADA, D. Formación y eliminación de burbujas en vidriados cerámicos, *Bol. Soc. Esp. Ceram.*, 1(8), 511-525, 1962.
- [2] ESCARDINO, A.; AMORÓS, J.L.; ORTS, M.J.; GOZALBO, A.; MESTRE, S.; APARISI, J. F.; FERRANDO, F.; SÁNCHEZ, L. Surface porosity of polished glazes. *C+CA*, 3-4, 97-110, 2003.
- [3] ORTS, M.J.; AMORÓS, J.L.; GARCÍA-TEN, J.; SÁNCHEZ, E.; GOZALBO, A. Propiedades superficiales del gres porcelánico: relación con la microestructura. *Técnica Cerámica*, 297, 1240-1248, 2001.
- [4] ESCARDINO, A. Vidriados cerámicos de naturaleza vitrocristalina. En: IV Congreso Mundial de la Calidad del Azulejo y del Pavimento Cerámico. Castellón. Cámara Oficial de Comercio, Industria y Navegación. Vol. I, 91-112, 1996.
- [5] PRADO, M.O. ZANOTTO, E.D. Glass sintering with concurrent crystallization. *C.R Chimie*, 5, 773-786, 2002.
- [6] REIJNEN, P.; FIRATLI, A.C.; GOERG, H.; ARSLAN, R. The mechanisms of pore growth during vitrification. *Cfi/Ber. DKG*, 61(8), 441-445, 1984.
- [7] LYON, K.C. Calculation of surface tensions of glasses. *J. Am. Ceram. Soc.*, 27(6), 186-189, 1944.